MST4 kinase phosphorylates ACAP4 protein to orchestrate apical membrane remodeling during gastric acid secretion

Received for publication, July 24, 2017 Published, Papers in Press, August 14, 2017, DOI 10.1074/jbc.M117.808212

Xiao Yuan[‡], Phil Y. Yao[§¶], Jiying Jiang[‡], Yin Zhang[‡§], Zeqi Su[‡§], Wendy Yao[¶1], Xueying Wang[‡], Ping Gui[‡], McKay Mullen[¶], Calmour Henry[¶2], Tarsha Ward[‡¶], Wenwen Wang[‡¶], Larry Brako[¶], Ruijun Tian[‡‖], Xuannv Zhao[§], Fengsong Wang[‡¶], Xinwang Cao[¶**], Dongmei Wang[‡], Xing Liu[‡¶3], Xia Ding[§4], and Xuebiao Yao[‡¶5]**

*From the [‡]BUCM-USTC Collaborative Center for Parietal Cell Research, CAS Center for Excellence in Molecular Cell Science, University of Science and Technology of China, Hefei 230027, China, the [§]Beijing University of Chinese Medicine, Beijing 100029, China, the [¶]Keck Center for Cellular Dynamics, Morehouse School of Medicine, Atlanta, Georgia 30310, the **Department of Biochemistry, Anhui Medical University, Hefei 230027, China, and the [‖]Southern University of Science and Technology, Shenzhen 518055, China*

Edited by Xiao-Fan Wang

Digestion in the stomach depends on acidification of the lumen. Histamine-elicited acid secretion is triggered by activation of the PKA cascade, which ultimately results in the insertion of gastric H,K-ATPases into the apical plasma membranes of parietal cells. Our recent study revealed the functional role of PKA–MST4–ezrin signaling axis in histamine-elicited acid secretion. However, it remains uncharacterized how the PKA–MST4–ezrin signaling axis operates the insertion of H,K-ATPases into the apical plasma membranes of gastric parietal cells. Here we show that MST4 phosphorylates ACAP4, an ARF6 GTPase-activating protein, at Thr^{545}. Histamine stimulation activates MST4 and promotes MST4 interaction with ACAP4. ACAP4 physically interacts with MST4 and is a cognate substrate of MST4 during parietal cell activation. The phosphorylation site of ACAP4 by MST4 was mapped to Thr^{545} by mass spectrometric analyses. Importantly, phosphorylation of Thr^{545} is essential for acid secretion in parietal cells because either suppression of ACAP4 or overexpression of non-phosphorylatable ACAP4 prevents the apical membrane reorganization and proton pump translocation elicited by histamine stimulation. In addition, persistent overexpression of MST4 phosphorylation-deficient ACAP4 results in inhibition of gastric acid secretion and blockage of tubulovesicle fusion to the apical membranes. Significantly, phosphorylation of Thr^{545} enables ACAP4 to interact with ezrin. Given the location of Thr^{545} between the GTPase-activating protein domain and the first ankyrin repeat, we reason that MST4 phosphorylation elicits a conformational change that enables ezrin–ACAP4 interaction. Taken together, these results define a novel molecular mechanism linking the PKA–MST4–ACAP4 signaling cascade to polarized acid secretion in gastric parietal cells.

The functions of an epithelium depend on the polarized organization of its individual epithelial cells. The establishment of a fully polarized phenotype and its plasticity control involve a cascade of complex events, including cell–cell adhesion, assembly of a lateral cortical complex, reorganization of the cytoskeleton, and polarized targeting of transport vesicles to the apical and basolateral membranes operated by a cascade of signaling transduction networks (1).

Mammalian MST4 kinase is a conserved element of the STE20 signaling cascade underlying cell polarity control (2). A recent study shows that MST4 phosphorylates ezrin at Thr^{567} at the apical membrane of intestinal cells, which induce brush borders (3). Ezrin is an actin-binding protein of the ezrin/radixin/moesin family of cytoskeleton–membrane linker proteins (4). Within the gastric epithelium, ezrin has been localized exclusively to parietal cells and primarily to the apical canalicular membrane of these cells (5, 6). Previous studies showed that gastric ezrin is co-distributed with the β-actin isoform *in vivo* (7) and preferentially bound to the β-actin isoform *in vitro* (8). It was postulated that ezrin couples the activation of PKA to the apical membrane remodeling associated with parietal cell secretion (5, 9). In fact, the PKA phosphorylation site on ezrin was mapped and demonstrated to be functionally important in histamine-elicited gastric acid secretion (5). Using mouse genetics, Tamura *et al.* (10) demonstrated that knocking down ezrin in the stomach to <5% of the wild-type level results in severe achlorhydria. In these parietal cells, H,K-ATPase–containing tubulovesicles failed to fuse with the apical membrane, suggesting an essential role of ezrin in tubulovesicle docking. Our recent studies showed that PKA cooperates with MST4 to orchestrate histamine-elicited acid secretion by phosphorylating ezrin at Ser^{66} and Thr^{567}, respectively (11). Histamine stimulation activates PKA, which phosphorylates MST4 at Thr^{178} and then promotes MST4 kinase activity. Our

This work was supported by National Key Research and Development Program of China Grants 2017YFA0503600 and 2016YFA0100500; Ministry of Education Grants IRT_17R102 and 20113402130010; Chinese Natural Science Foundation Grants 31430054, 31621002, 81630080, 31501095, 31271518, and 31501130; Strategic Priority Research Program of Chinese Academy of Sciences Grant XDB19000000; National Institutes of Health Grants CA164133, DK115812, and DK56292; and Central University Grant WK2070000066. The authors declare that they have no conflicts of interest with the contents of this article. The content is solely the responsibility of the authors and does not necessarily represent the official views of the National Institutes of Health.

[1] An American Digestive Health Foundation student research fellow.
[2] Awarded a summer research fellowship of the Morehouse School of Medicine.
[3] To whom correspondence may be addressed. E-mail: xing1017@ustc.edu.cn.
[4] To whom correspondence may be addressed. E-mail: dingx@bucm.edu.cn.
[5] To whom correspondence may be addressed. E-mail: xyao@msm.edu.

studies show that MST4 is important for acid secretion in parietal cells because either suppression of MST4 or overexpression of non-phosphorylatable MST4 prevents the apical membrane reorganization and proton pump translocation elicited by histamine stimulation. However, it was unclear how MST4 activity is orchestrated and links to tubulovesicle fusion to the apical membrane and concomitant remodeling of the apical membrane during parietal cell activation.

Our early studies revealed that ezrin interacts with ACAP4, an ADP ribosylation factor 6 (ARF6)[6] GTPase-activating protein (GAP) containing a Bin, Amphiphysin, and RSV161/167 domain, a pleckstrin homology domain, an ARFGAP domain, and ankyrin repeats, in a context-dependent manner (12). ACAP4 locates in the cytoplasmic tubulovesicle membrane in resting parietal cells but translocates to the apical plasma membrane upon histamine stimulation. Importantly, ezrin specifies the apical distribution of ACAP4 in secreting parietal cells because either suppression of ezrin or overexpression of non-phosphorylatable ezrin prevents the apical localization of ACAP4. Although these results define a novel molecular mechanism linking ACAP4 – ezrin interaction to polarized epithelial secretion, it was undetermined whether MST4 activity regulates ACAP4 activation and how MST4 orchestrates tubulovesicle trafficking to the apical membrane during parietal cell activation.

Here we show that ACAP4 is downstream from MST4 during parietal cell activation. MST4 phosphorylates ACAP4 at Thr^{545}, which is essential for parietal cell acid secretion. Importantly, Thr^{545} is located between GAP domain and the first ankyrin repeat. We reason that MST4-induced phosphorylation of Thr^{545} elicits a conformational change to enable ACAP4 binding to ezrin phosphorylated by PKA. Thus, our study provides novel insight into the PKA–MST4 –ACAP4 signaling axis in polarized membrane trafficking in stimulus-coupled acid secretion in parietal cells.

Results

Identification of a novel MST4 –ACAP4 complex in secreting gastric parietal cells

Our previous studies revealed the functional importance of ACAP4 in membrane cytoskeletal dynamics during stimulus-coupled membrane remodeling (12–14). Because ACAP4 relocates from the cytoplasm to the apical plasma membrane during gastric parietal cell activation, we sought to examine the role of ACAP4 in stimulus-coupled parietal cell activation. To study the molecular association of ACAP4 with other accessory proteins, we carried out affinity isolation of an ACAP4-containing protein complex followed by mass spectrometric identification of tryptic peptides derived from the complex, as described previously (12, 15, 16). Specifically, an ACAP4 affinity matrix was used to isolate the ACAP4-associated large-mass complex in histamine-stimulated parietal cells. As shown in Fig. 1*A*, anti-ACAP4 affinity beads coupled to an anti-ACAP4 antibody isolated a major polypeptide of 99 kDa in addition to three visible bands of polypeptides with approximate masses of 55 kDa, 45 kDa and 25 kDa, respectively (Fig. 1*A*, *lane 1*). The 45-kDa polypeptide was absent from the ACAP4 antibody affinity matrix incubated with non-secreting (NS) parietal cell lysates (Fig. 1*A*, *lane 2*) and was confirmed as MST4 based on mass spectrometry and Western blot analyses (Fig. 1*A*, *bottom panel*, *lane 1*). Our mass spectrometric analyses identified the 45-kDa polypeptide as MST4, a characterized cell polarity kinase interacting with ezrin in cell polarity establishment and parietal cell acid secretion (11). Western blotting analyses validated that the actin-binding protein ezrin also exists in the immunoprecipitates of ACAP4 in secreting parietal cells (Fig. 1*B*, *lane 3*) but not non-secreting parietal cells (Fig. 1*B*, *lane 4*). As a negative control, tubulin was absent from ACAP4 immunoprecipitates (Fig. 1*B*, *lanes 3* and *4*).

The cortical cytoskeleton constitutes an important subcellular structure that determines cell shape and orchestrates cellular dynamics. Ezrin is a signaling scaffold protein located on the apical membrane of polarized epithelial cells for integration of diverse signaling pathways. The identification of MST4 and ezrin in the ACAP4 protein complex prompted us to validate the interaction of MST4 –ACAP4 using reciprocal immunoprecipitation, in which MST4 antibody isolated ACAP4 only from secreting parietal cells but not from non-secreting cells (Fig. 1*C*, *lanes 3* and *4*). We next examined whether MST4 is co-localized with ACAP4 in gastric parietal cells. To this end, we carried out immunofluorescence microscopic analyses of isolated gastric glands doubly stained for ACAP4 and MST4. As shown in Fig. 1*D*, ACAP4 distributes in the cytoplasm of gastric parietal cells (*a′*, *white arrowheads*). ACAP4 and MST4 are absent from non-parietal cells such as gastric chief cells (Fig. 1*D*, *a′* and *b′*, *yellow arrows*). Interestingly, this parietal cell–selective localization of ACAP4 is largely superimposed onto that of MST4 when two channels were merged (Fig. 1*D*, *c′*, *white arrowheads*). Phase-contrast imaging of the same gastric glands confirmed the preferential enrichment of ACAP4 and MST4 in gastric parietal cells (Fig. 1*D*, *d′*). Interestingly, an enlarged montage from merged images suggested a partial co-distribution of ACAP4 with MST4 within parietal cells (Fig. 1*D*, *c′*). Thus, we conclude that ACAP4 interacts and co-distributes with MST4 in gastric parietal cells.

Thr^{545} of ACAP4 is a cognate substrate of MST4

Our recent work has established the essential role of MST4 in gastric parietal cell activation (11). Identification of the stimulation-elicited MST4 –ACAP4 interaction prompted us to examine whether ACAP4 is a substrate of MST4 during parietal cell activation. To this end, we isolated the ACAP4 protein band from SDS-PAGE shown in Fig. 1*A* and subjected it for phosphorylation site mapping using mass spectrometric analyses. A resulting peptide containing $pThr^{545}$ (addition of a phospho group with neutral loss of a water molecule) was resolved by MS-MS (b- and y-series ions are labeled). As shown in Fig. 2*A*, the prominent b-series ions b3, 5, 6, and 7 and y-series ions y6 and y7 present unambiguous evidence for $pThr^{545}$.

Our mass spectrometric analyses of $pThr^{545}$ of ACAP4 suggest that it is a potential substrate for MST4 kinase. Computational analyses of ACAP4 structural domains reveal that Thr^{545} is located between the GAP domain and ankyrin repeat of

[6] The abbreviations used are: ARF, ADP ribosylation factor; GAP, GTPase-activating protein; NS, non-secreting; SLO, Streptolysin O; AP, aminopyrine; MEM, minimal essential medium; IBMX, isobutylmethylxanthine.

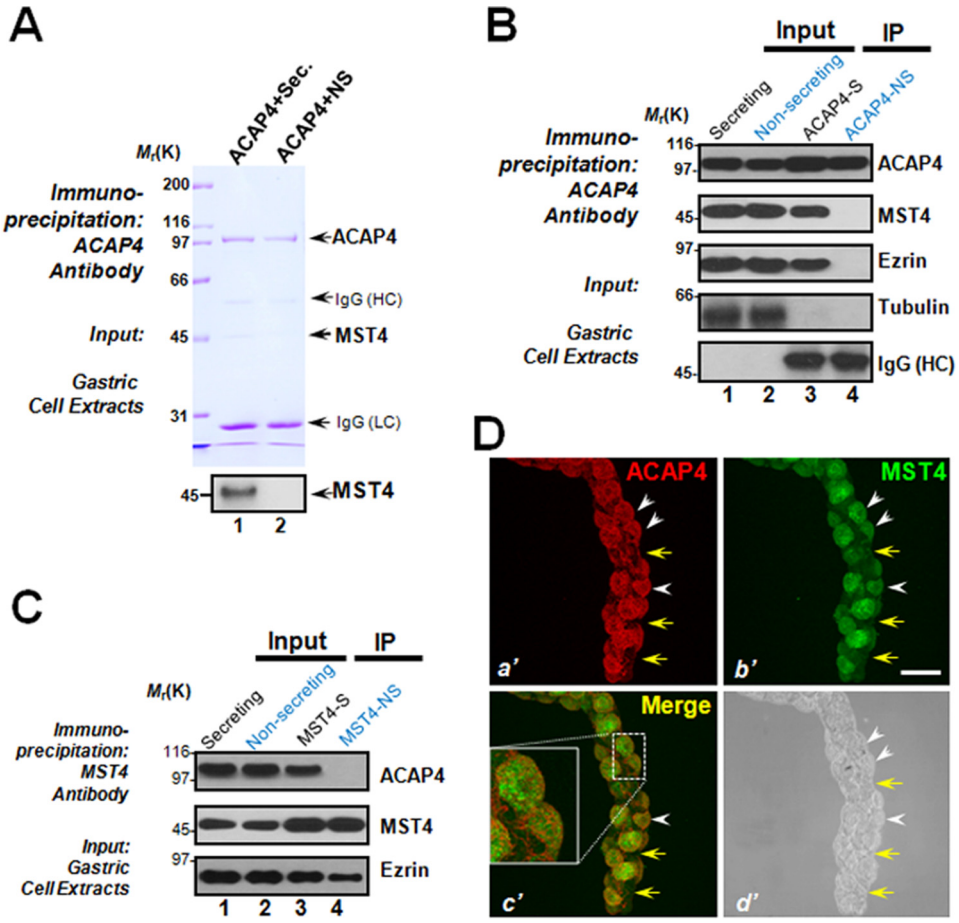

Figure 1. ACAP4 is a novel MST4 interaction partner in histamine-stimulated gastric parietal cells. *A*, ACAP4 forms a novel complex with MST4 in secreting parietal cells. Aliquots of secreting (histamine-treated) and NS gastric parietal cells were collected by centrifugation and extracted with Triton X-100–containing buffer as described under "Experimental procedures." Clarified cell lysates were incubated with Sepharose bead affinity matrix covalently coupled with ACAP4 mouse antibody as described under "Experimental procedures." The beads were washed successively with PBS before elution with 0.2 M glycine (pH 2.3). All samples were separated by SDS-PAGE. The ACAP4 protein band migrating at 99 kDa along with the 45-kDa bands were then removed for mass spectrometric identification. Western blot analysis confirmed that the 45-kDa band is MST4 (*bottom panel*). *HC*, heavy chain; *LC*, light chain. *B*, ACAP4 immunoprecipitates (*IP*) from secreting and non-secreting gastric parietal cells were immunoblotted with antibodies against ACAP4, MST4, ezrin, and tubulin. Note that only ACAP4 immunoprecipitates from secreting parietal cells brought down ezrin and MST4 but not tubulin. Neither ezrin nor MST4 were observed in ACAP4 immunoprecipitates from non-secreting parietal cells. *C*, MST4 immunoprecipitates from secreting and non-secreting gastric parietal cells were immunoblotted with antibodies against ACAP4, MST4, and ezrin. Note that only MST4 immunoprecipitates from secreting parietal cells brought down ACAP4. *D*, isolated gastric glands were labeled with antibodies against ACAP4 (*a'*, *red*), MST4 (*b'*, *green*) and imaged for phase contrast (*d'*). Images from ACAP4 (*a'*, *red*) and MST4 (*b'*, *green*) were merged to assess their co-distribution profiles in gastric glandular cells (*c'*). *Scale bar* = 10 μm. Note that ACAP4 is co-localized to the corresponding MST4-positive gastric parietal cells (*white arrowheads*) but not non-parietal cells (*yellow arrows*).

ACAP4 (Fig. 2*B*). To test whether Thr^{545} is a substrate of MST4, we performed *in vitro* phosphorylation on recombinant His_6–ACAP4 fusion proteins, including both wild-type ACAP4 and a mutant ACAP4 in which Thr^{545} was replaced by alanine (T545A). Both histidine fusion proteins, wild-type and the Thr^{545}-mutated ACAP4 mutant ($ACAP4^{T545A}$), migrate at about the predicted 99 kDa, as shown in Fig. 2*C* (*top panel*, Coomassie Blue staining). Incubation of the fusion proteins with [γ-^{32}P]ATP and MST4 resulted in incorporation of ^{32}P into the wild type but not the $ACAP4^{T545A}$ mutant (Fig. 2*C*, *bottom panel*, *lanes 2* and *3*). This MST4-mediated phosphorylation is specific because incubation of MST4 with [γ-^{32}P]ATP in the presence of 20 nM hesperadin, a chemical inhibitor of MST4 (17), resulted in undetectable incorporation of radioactivity into the wild-type protein (Fig. 2*C*, *bottom panel*, *lane 1*). Quantitative analyses showed that incorporation of ^{32}P into ACAP4 is a function of MST4 (Fig. 2*D*). Thus, Thr^{545} of ACAP4 is a *bona fide* substrate for MST4.

Phosphorylation of Thr^{545} of ACAP4 is essential for parietal cell activation

Because parietal cell activation involves ezrin-mediated reorganization of the apical membrane cytoskeleton (11), we sought to probe the localization of ACAP4 using immunofluorescence microscopy. As shown in Fig. 3*A*, *a'*, ACAP4 is primarily localized to the cytoplasm of parietal cells treated with cimetidine as a diffused signal. However, ACAP4 is enriched in the apical membrane as two interconnected and dilated rings in a single cell in response to histamine stimulation (Fig. 3*A*, *b'*). To evaluate the functional importance of ACAP4 phosphorylation in parietal cell secretion, we adopted apical vacuole diameter (Fig. 3*B*, *Apical Dia.*) as a reporter for parietal cell secretory activity (18). Quantitative analyses of 100 parietal cells from cimetidine and histamine treatment, as summarized in Fig. 3*B*, demonstrated that stimulation dramatically extended the apical vacuole diameter to 15.7 ± 0.9 μm, whereas the average vacuole

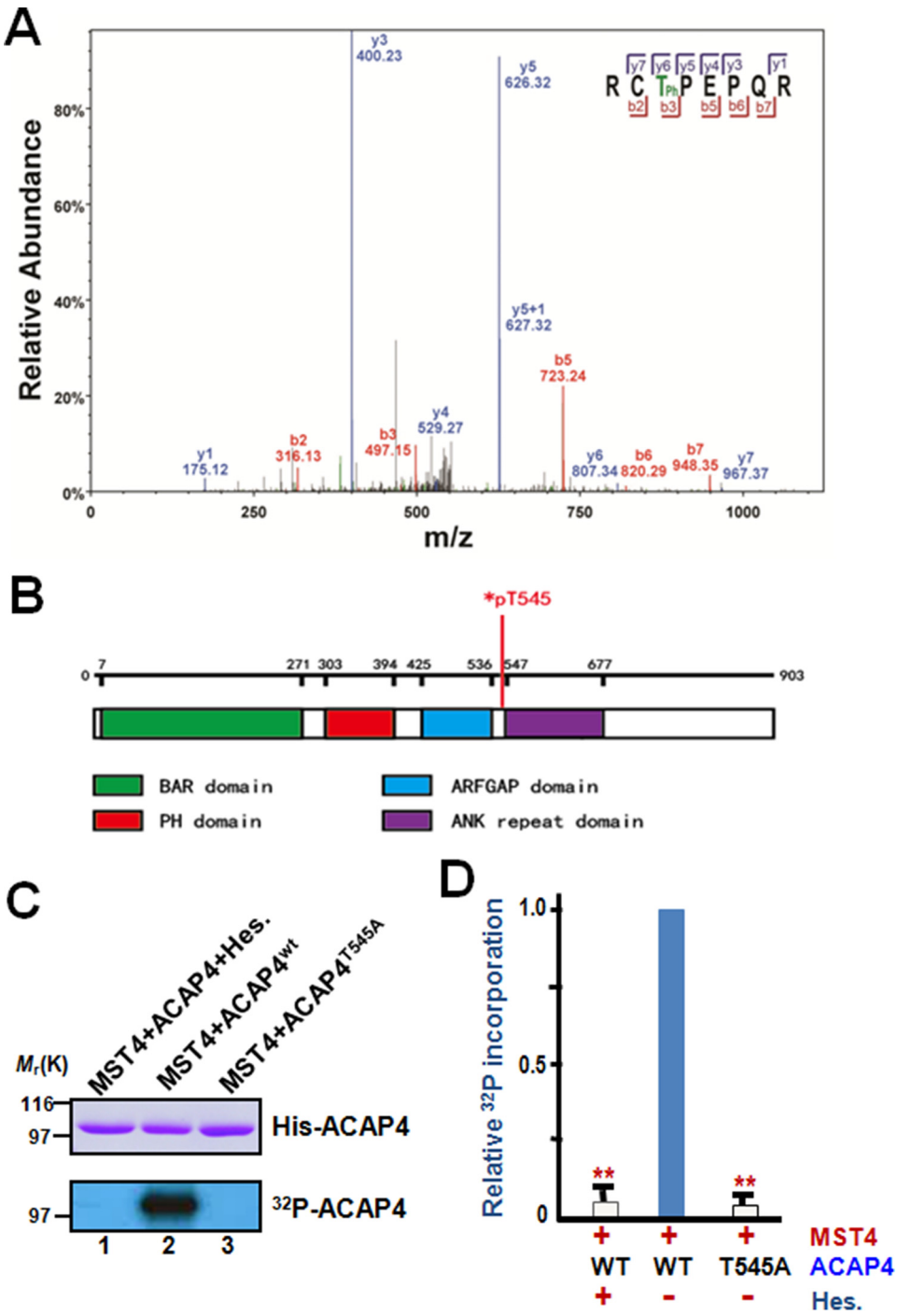

Figure 2. ACAP4 is a novel substrate of MST4 and is phosphorylated during parietal cell secretion. *A*, representative phosphopeptide mass spectrum from ACAP4 isolated from secreting parietal cells. A representative band from SDS-PAGE shown in Fig. 1*A* (*lane 1*) was removed for trypsin digestion followed by mass spectrometric analyses as detailed under "Experimental procedures." The annotated spectra from mass spectrometric analyses indicate that ACAP4 is phosphorylated at Thr^{545} in secreting parietal cells. *B*, schematic illustrating the functional domains of ACAP4 and annotating the location of $pThr^{545}$. *C*, Thr^{545} of ACAP4 is a substrate of MST4 *in vitro*. Aliquots of recombinant His_6-tagged ACAP4 were purified and incubated with MST4 or MST4 plus its chemical inhibitor hesperadin (*Hes.*) as detailed under "Experimental procedures." As a control, we used an aliquot of recombinant ACAP4 with the putative MST4 site mutated to alanine ($ACAP4^{T545A}$, *lane 3*). *Top panel*, Coomassie Blue–stained SDS-PAGE. *Bottom panel*, ^{32}P incorporation from the same gel. *D*, quantitative analyses of *in vitro* phosphorylation efficiency in *C*. **, $p < 0.01$ compared with wild-type ACAP4 controls. *Error bars* represent the standard error of three separate preparations.

diameter of cimetidine cells was only 2.3 ± 0.5 μm, which represents ~14.6% of maximal secretory activity. Pretreatment with hesperadin abolished the histamine-elicited apical dilation (24.3% ± 5.3% of maximal dilation), consistent with the role of MST4 in parietal cell activation (Fig. 3*B*; **, $p < 0.01$). The measurement of apical vacuole diameter as parietal cell activation is consistent with the secretary activity assay of aminopyrine (AP) uptake, which quantifies gastric acid secretion (Fig. 3*B*). We therefore reason that MST4 is essential for the dynamic translocation of ACAP4 and remodeling of the apical

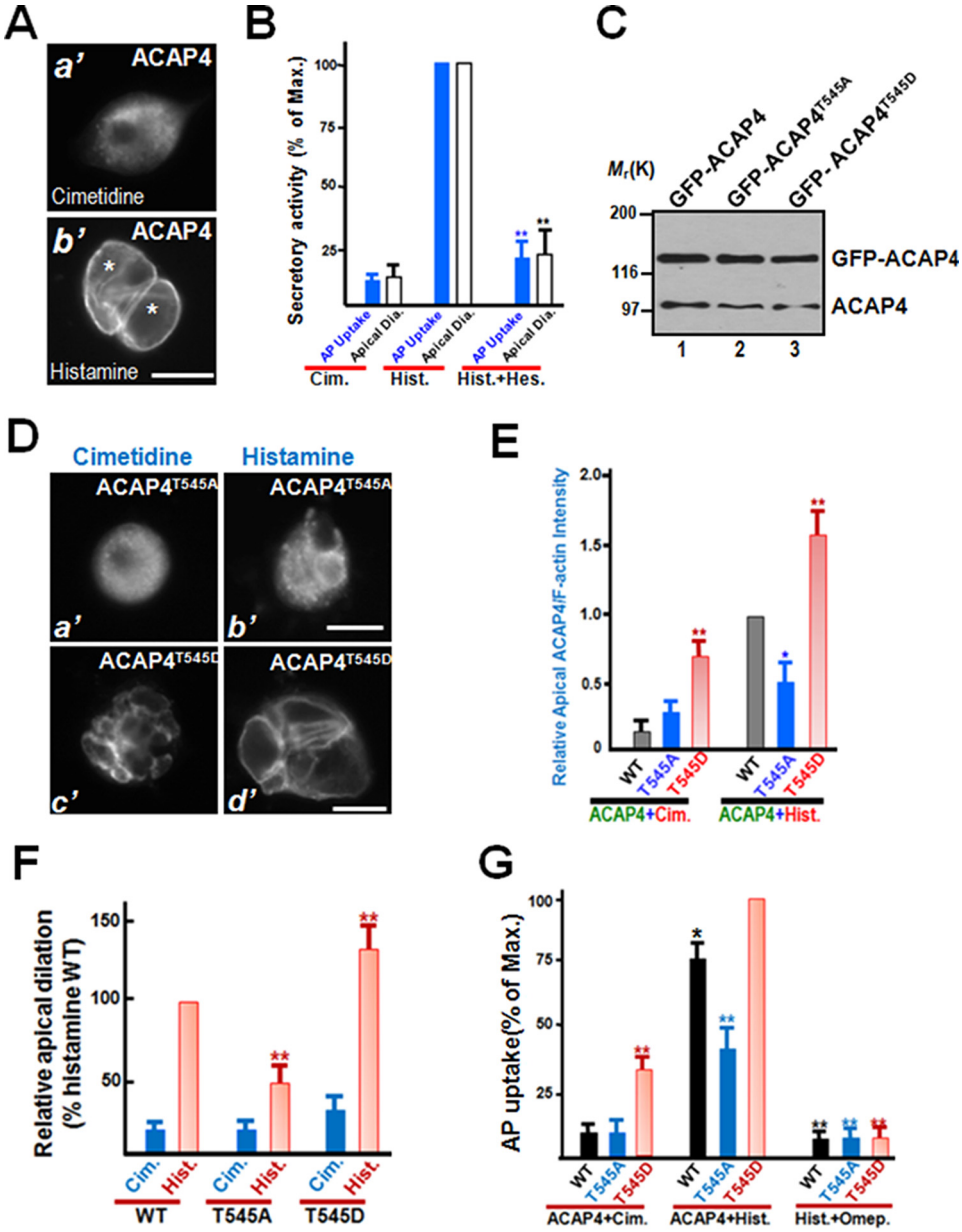

Figure 3. MST4-elicited phosphorylation of Thr^{545} is essential for parietal cell activation. *A*, immunofluorescence staining of ACAP4 in non-secreting and secreting cultured parietal cells. ACAP4 is primarily located to the cytoplasm, with brief concentration at the apical membrane. However, after histamine stimulation, the ACAP4 signal is enriched in dilated apical membrane vacuoles. *Scale bar* = 10 μm. *B*, quantitative analyses of apical vacuole diameter as a function of parietal cell secretion. In parallel to morphological quantification of apical vacuole diameter as a function of parietal cell secretion, aliquots of gastric parietal cells were treated with cimetidine (*Cim.*), histamine (*Hist.*), and hesperadin (*Hes.*) plus histamine at 37 °C for 20 min as described under "Experimental procedures," followed by assessment of secretory activity using AP uptake. **, $p < 0.01$ compared with histamine-stimulated controls. *Max.*, maximal stimulation. *Error bars* represent the standard error of three separate preparations in each category. In the case of quantification of apical vacuole diameter (*white columns*), *error bars* represent the standard error of three separate preparations of 20 cells in each category. *C*, characterization of expression of GFP–ACAP4 proteins in gastric parietal cells. Aliquots of parietal cells were transiently transfected to express ACAP4 proteins (wild-type, T545A, and T545D). Twenty-four hours after transfection, cell lysates were prepared and fractionated on SDS-PAGE, followed by Western blot analyses with ACAP4 antibody. Note that the exogenous GFP–ACAP4 proteins expressed 3-fold higher compared with endogenous ACAP4. *D*, MST4-elicited phosphorylation of ACAP4 at Thr^{545} orchestrates histamine stimulation. Aliquots of parietal cells were transiently transfected to express ACAP4 proteins (T545A and T545D). 24 h after transfection, the parietal cells were treated with histamine (100 μM) as detailed under "Experimental procedures," followed by fixation and immunofluorescence analyses. Note that the exogenous ACAP4^{T545D}-expressing cells exhibited larger apical membrane vacuoles even before histamine stimulation. *Scale bars* = 10 μm. *E*, quantitative analyses of apical localization of ACAP4-expressing (WT, phospho-mimicking T545D, non-phosphorylatable T545A) parietal cells as a function of activation. *, $p < 0.05$; **, $p < 0.01$ compared with those of wild-type ACAP4-expressing cells in secreting and non-secreting status. *Error bars* represent the standard error of three separate preparations of 20 cells in each category. *F*, quantitative analyses of apical vacuole diameter of ACAP4-expressing parietal cells as a function of activation. **, $p < 0.01$ compared with stimulated controls. *Error bars* represent the standard error of three separate preparations of 50 cells in each category. Typically, the average diameter of apical vacuoles in cimetidine-treated non-secreting parietal cells is 2.9 $\pm$ 0.3 μm, whereas the diameter for histamine-stimulated secreting cells is 15.7 $\pm$ 1.1 μm. The transfection efficiency is 50–55%, as judged by the GFP signal in transfected preparations under a microscope. *G*, MST4 phosphorylation of ACAP4 cooperates with PKA activation for optimal parietal cell activation. Aliquots of gastric parietal cells were transiently transfected to express ACAP4 wild-type and phosphomutants, and transfected cells were subjected to assess secretory activity using an AP uptake assay as described under "Experimental procedures." Aliquots of the proton pump inhibitor omeprazole (100 nM) were included to validate whether histamine-stimulated and ACAP4-dependent acid secretion is mediated by proton pump H,K-ATPase. Note that omeprazole treatment inhibited ACAP4 T545D-dependent acid secretion in response to histamine stimulation. **, $p < 0.01$; *, $p < 0.05$ compared with stimulated controls. *Error bars* represent the standard error of three separate preparations.

membrane of parietal cells associated with the stimulation of gastric acid secretion.

To evaluate the role of MST4-elicited phosphorylation of ACAP4 in parietal cell activation, we attempted to transiently transfect cultured parietal cells for expressing exogenous ACAP4. To test the efficiency of exogenous ACAP4 expression, cultured parietal cells were transfected with GFP-tagged wild-type and phosphorylation-mutant ACAP4 plasmids. Western blot analysis carried out using transfected cells showed that exogenously expressed ACAP4 proteins were about 2.5- to 3.1-fold higher than the level of endogenous ACAP4 in cultured parietal cells (Fig. 3*C*). Assuming a transfection efficiency of about 50–55%, the actual expression level of GFP-ACAP4 in positively transfected cells is about 5-fold higher than that of endogenous protein.

Parietal cell activation exhibits characteristic translocation of H,K-ATPase from tubulovesicles to the apical membrane; therefore, we sought to examine parietal cell activation in phospho-mimicking ACAP4 (GFP-ACAP4^{T545D})-expressing and non-phosphorylatable ACAP4 (GFP-ACAP4^{T545A})-expressing cells, respectively. The transfected cells were then treated with either cimetidine or histamine before being fixed for immunofluorescence microscopic analyses. As shown in Fig. 3*D*, although GFP-ACAP4^{T545A} is primarily localized to the cytoplasm of cimetidine-treated cells (*a′*), it becomes relocated to the apical plasma membrane in response to histamine stimulation (*b′*). Consistent with our speculation, expression of phospho-mimicking ACAP4 (ACAP4^{T545D}) resulted in expansion of the apical membrane in parietal cells (Fig. 3*D*, *c′*), as the majority of ACAP4^{T545D} is concentrated at the apical membrane of parietal cells. ACAP4^{T545D}-expressing cells produce characteristic vacuolar swelling in response to histamine stimulation (Fig. 3*D*, *d′*), suggesting a potential role of MST4 activation in recruiting H,K-ATPase–containing vesicles to the apical membrane. Quantitative analyses demonstrated that ACAP4 is relocated to the apical membrane in response to histamine-elicited MST4 activation (Fig. 3*E*). Dilation of apical vacuoles is a characteristic of secreting parietal cells (5). Typically, the average diameter of apical vacuoles in cimetidine-treated, non-secreting parietal cells is 2.9 ± 0.3 μm, whereas the diameter for histamine-stimulated secreting cells is 15.7 ± 1.1 μm, consistent with previous studies (5, 19). The vacuolar measurements, summarized in Fig. 3*F*, indicate that abrogation of MST4-elicited ACAP4 phosphorylation prevents the histamine-elicited apical vacuole dilation seen in ACAP4^{T545A}-expressing cells. We therefore reason that MST4–ACAP4 interaction is essential for the dynamic remodeling of the apical plasma membrane of parietal cells associated with the stimulation.

The functional importance of ACAP4 phosphorylation in parietal cell secretion prompted us to examine the precise function of MST4–PKA interaction in parietal cell activation. To directly probe for the function of MST4–ACAP4 interaction, we sought to introduce wild-type and mutant ACAP4 (T545A and T545D) into cultured parietal cells by transient transfection (12, 19, 20). As predicted, histamine stimulation of wild-type ACAP4-expressing cells produced dramatic acid secretion, as judged by AP uptake (Fig. 3*G*). However, the ACAP4^{T545A} mutant inhibited histamine-elicited parietal cell secretion, whereas ACAP4^{T545D} synergizes with histamine, which resulted in maximal acid secretion equivalent to 125% of that seen in wild type–expressing cells. This secretory activity is dependent on H,K-ATPase, as treatment with the proton pump inhibitor omeprazole (100 nM) abolished histamine stimulation of acid secretion (Fig. 3*G*). These results suggest that ACAP4 cooperates with MST4 for maximal parietal cell secretion via phosphorylating ACAP4 at Thr^{545} and that acid secretion is dependent on proton pump H,K-ATPase.

Phosphorylation of Thr^{545} by MST4 elicits ACAP4 binding to Ser^{66}-phosphorylated ezrin

The crystal structure reveals that the linker region between the ankyrin repeat and GAP domain exhibits great flexibility to bridge compact lobes. Thr^{545} resides in the flexible loop, based on the molecular modeling shown in Fig. 4*A*. We speculate that phosphorylation of Thr^{545} elicits a conformational change of ACAP4 to enable the interaction of MST4 with ACAP4. To test this hypothesis, we performed *in vitro* binding assays in which phosphorylated and non-phosphorylatable ACAP4 proteins were used as inputs to test for its ability to bind to the affinity matrix containing ezrin proteins (S66A and S66D; Fig. 4*B*, *lanes 3–7*). As shown in Fig. 4*B*, the His_6-tagged ezrin S66A and S66D proteins migrate at about the predicted 80 kDa (*top panel*, Coomassie Blue staining). Non-phosphorylatable ACAP4 failed to bind to S66A and S66D affinity beads (Fig. 4*B*, *lanes 4* and *6*). Interestingly, phosphorylation-mimicking ACAP4 was only retained on S66D affinity matrix (Fig. 4*B*, *lane 5*), indicating a context-dependent association between ACAP4 and ezrin. The Western blot analyses confirmed this phosphorylation-dependent ACAP4 association with ezrin. Consistent with the notion of phosphorylation-dependent ACAP4–ezrin association, phosphorylation-mimicking ACAP4 failed to be retained on the wild-type ezrin affinity matrix, as judged by Western blot analyses (Fig. 4*C*, *bottom panel*, *lane 4*). This context-dependent ACAP4 association with phosphorylated ezrin was also confirmed using an immunoprecipitation assay (Fig. 4*D*). Thus, we conclude that MST4 phosphorylation of ACAP4 at Thr^{545} enables ACAP4 binding to ezrin.

To directly probe for the function of phosphorylation-dependent MST4–ACAP4 interaction in parietal cell activation, we sought to introduce wild-type and mutant ACAP4 (T545A and T545D) together with wild-type and mutant ezrin (S66A and S66D) into SLO-permeabilized parietal cells to mimic PKA phosphorylation *in vivo* using a protocol reported previously (12, 19, 20). As shown in Fig. 4*E*, addition of recombinant ezrin^{S66D} together with ACAP4^{T545D} produced maximal stimulation of acid secretion, whereas S66D or T545D alone only gave a mean stimulation value about 75% of maximal secretion (**, $p < 0.01$). Consistent with previous studies, non-phosphorylatable ezrin (S66A) prevents cAMP-elicited parietal cell secretion, as there is no secretion in the presence of ATP, as judged by AP uptake. In addition, non-phosphorylatable ACAP4 (T545A) prevents cAMP-elicited parietal cell secretion, consistent with the role of the PKA–MST4–ACAP4 signaling axis in parietal cell activation. Importantly, this cAMP-elicited and T545D-dependent parietal cell secretion was reduced to 41.7% of maximal secretion upon treatment with the

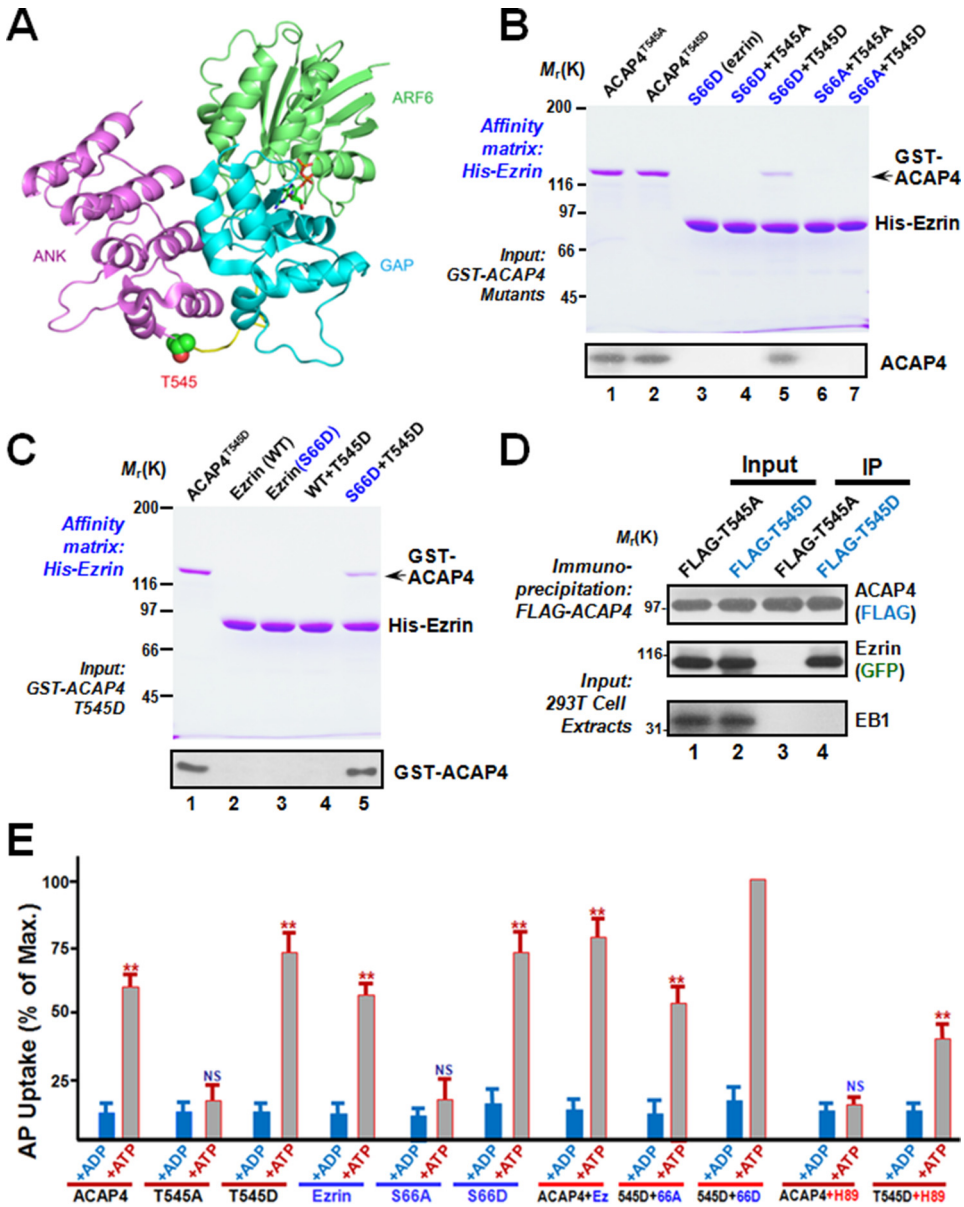

Figure 4. Phosphorylation of Thr^{545} is essential for ACAP4 – ezrin interaction and parietal cell acid secretion. *A*, a canonical ARF–ARFGAP complex (PDB code 3LVQ) structure shown as a schematic with ARF6 in *green*, the GAP domain in *cyan*, and the ANK repeat in *purple*. The linker between the ACAP4 GAP domain and ankyrin repeat is colored in *yellow*. The Thr^{545} side chain important for phosphorylation is represented as *spheres*. The figure was generated by PyMOL software (The PyMOL Molecular Graphics System, version 1.8 Schrödinger, LLC). *B*, phosphorylation of ACAP4 at Thr^{545} specifies its association with ezrin. Various His$_6$–ezrin proteins were purified on nickel-nitrilotriacetic acid beads, followed by incubation with GST-ACAP4^{T545D} and GST-ACAP4^{T545A} proteins. Beads were washed and boiled in SDS-PAGE sample buffer, followed by SDS-PAGE analyses of proteins bound to the beads. Western blotting analyses, shown in the *bottom panel*, confirmed that ACAP4^{T545D} selectively binds to Ezrin^{S66D}. *C*, phosphorylation of Thr^{545} of ACAP4 specifies its association with phospho-mimicking ezrin^{S66D}. Both wild-type and phospho-mimicking ezrin^{S66D} proteins were purified on nickel-nitrilotriacetic acid beads, followed by incubation with GST-ACAP4^{T545D} protein. Beads were washed and boiled in SDS-PAGE sample buffer, followed by SDS-PAGE analyses of proteins bound to the beads. Western blotting analysis, shown in the *bottom panel*, confirmed that ACAP4 ^{T545D} selectively binds to ezrin^{S66D} but not wild-type ezrin. *D*, phosphorylation of Thr^{545} of ACAP4 specifies its association with ezrin in 293T cells. An immunoprecipitation (*IP*) assay was used to demonstrate the complex formed by ACAP4^{T545D} and ezrin in cultured cells. Note that ACAP4^{T545A} failed to form a complex with ezrin. *E*, phosphorylation of Ser^{66} on ezrin and Thr^{545} on ACAP4 synergize for parietal cell secretion. Gastric glands were SLO-permeabilized and incubated with various recombinant ezrin mutants mimicking Ser^{66} phosphorylation independently or as combination with ACAP4 mutants mimicking Thr^{545} phosphorylation before being stimulated with 100 μM cAMP plus 100 μM ATP, and AP uptake was measured as described under "Experimental procedures." AP uptake was plotted as a percentage of the stimulated control for each experiment. *Error bars* represent S.E.; $n = 5$. *, significant difference from stimulated controls (**, $p < 0.01$); *NS*, no significant difference. Note that ezrin mutant mimicking Ser^{66} phosphorylation combined with ACAP4 mutant mimicking Thr^{545} phosphorylation exhibited greatest secretory activity in response to cAMP stimulation. cAMP-elicited ACAP4-dependent parietal cell secretion is inhibited by the PKA inhibitor H89.

PKA inhibitor H89 (Fig. 4*E*; **, $p < 0.01$), indicating that PKA activity is required for ACAP4-mediated acid secretion. Therefore, we conclude that MST4-elicited phosphorylation of ACAP4 cooperates with PKA-activated ezrin to orchestrate maximal stimulation of acid secretion.

Phosphorylation of Thr^{545} is essential for recruitment of tubulovesicles to the apical plasma membrane

From a resting state to a secreting state, there are major changes at the apical canalicular surface, including elongation of microvilli and expansion of the apical and canalicular mem-

branes because of the recruitment of tubulovesicles (21, 22). Several lines of studies demonstrate that ezrin is the linker between actin filaments and the apical plasma membrane in gastric parietal cells, as suppression or perturbation of ezrin integrity resulted in failure to remodel the apical and canalicular membranes (20) and hypochlorhydria in mice (10). Given the physical interaction between ACAP4^{T545D} and ezrin^{S66D}, we hypothesize that MST4-elicited phosphorylation of ACAP4 is essential for recruitment of tubulovesicles to the apical membrane. To test this hypothesis, we carried out electron microscopy examination of gastric parietal cells overexpressing ACAP4^{T545D} and ACAP4^{T545A}, followed by histamine stimulation. In typical control experiments of cimetidine treatment, wild-type ACAP4-expressing parietal cells exhibited the typical resting morphology: few canalicular profiles with short microvilli and numerous tubulovesicles (*e.g.* Ref. 20). On stimulation by histamine, a dramatic change occurred in the form of elaborate canaliculi with long microvilli, and the tubulovesicles became rare, as typically reported for histamine-activated parietal cells (8, 20). A representative micrograph of ACAP4^{T545D}-expressing parietal cells is shown in Fig. 5*A*, and in this micrograph, expanded canaliculi are readily apparent (*red asterisks*). The greatly expanded canalicular membrane and elongated microvilli in proximity to the plasma membrane can clearly be seen (Fig. 5*B*, *a*, *asterisk*). There are virtually no tubulovesicles in proximity to the plasma membrane of ACAP4^{T545D}-expressing cells (Fig. 5*B*; *a* and *b*). Careful examination revealed a few tubulovesicles in proximity to the canalicular membrane of ACAP4^{T545D}-expressing cells (Fig. 5*B*, *b*, *yellow arrow*). However, this characteristic canalicular membrane expansion was minimized in histamine-stimulated ACAP4^{T545A}-expressing cells (Fig. 5*C*). In addition, there is a great abundance of tubulovesicles in proximity to the plasma membrane of ACAP4^{T545A}-expressing cells (Fig. 5*D*, *a* and *b*). Careful examination revealed dozens of tubulovesicles in close proximity to the canalicular membrane of ACAP4^{T545A}-expressing cells (Fig. 5*D*, *a* and *b*, *yellow arrows*), indicating that non-phosphorylatable ACAP4 failed to support recruitment of the tubulovesicular membrane to the apical plasma membrane during histamine stimulation. We surveyed 120 cross-sections from 10 different cells, which display a defined arrangement of canaliculi and tubulovesicles in both ACAP4^{T545A}-expressing and ACAP4^{T545D}-expressing parietal cells. As shown in Fig. 5*E*, ACAP4^{T545A} expression significantly increased the number of tubulovesicle in proximity to the canalicular membrane (10 ± 2 per μm^2), whereas wild-type ACAP4-expressing and ACAP4^{T545D}-expressing preparations only contained a few tubulovesicles in proximity to the canalicular membrane (3 ± 1 per μm^2 and 2 ± 1 per μm^2, respectively; **, $p < 0.01$). Thus, we conclude that MST4-elicited phosphorylation of Thr^{545} on ACAP4 is essential for recruitment of tubulovesicles to the apical membrane during parietal cell activation (Fig. 5*F*).

Phosphorylation of Thr^{545} is required for relocation of H,K-ATPase to the apical plasma membrane

Because parietal cell activation is hallmarked by the translocation of proton pump H,K-ATPase from tubulovesicles to the apical membrane, we sought to assess the translocation of H,K-ATPase in non-phosphorylatable ACAP4-expressing cells. To this end, cultured rabbit parietal cells were stimulated with histamine, followed by subcellular fractionation and differentiated centrifugation, as illustrated in our recent studies (11, 18). Western blot analyses indicate that the H,K-ATPase α subunit (~97-kDa polypeptide) is redistributed to the apical plasma membrane upon histamine stimulation (Fig. 6*A*, *lanes 1* and *2*). To test whether phosphorylation of ACAP4 Thr^{545} is involved in ezrin-mediated docking and partition of H,K-ATPase to the apical membrane of parietal cells, we performed the aforementioned fractionation experiment using cultured parietal cells infected with adenoviral GFP-ACAP4 (wild-type, phosphomimicking mutant and non-phosphorylatable mutant) for 8 h, followed by histamine stimulation. As shown in Fig. 6*B*, histamine-stimulated translocation of H,K-ATPase in wild-type GFP-ACAP4 – expressing cells exhibits a typical translocation of H,K-ATPase from tubulovesicle-enriched fraction P3 to plasma membrane-enriched fraction P1 (compare *lanes 3* and *4* with *lanes 1* and *2*). Interestingly, histamine failed to induce translocation of H,K-ATPase in non-phosphorylatable ACAP4^{T545A}-infected (Fig. 6*B*, *lanes 5* and *6*) but not phosphomimicking ACAP4^{T545D}-infected cells (Fig. 6*B*, *lanes 7* and *8*), demonstrating that ACAP4 phosphorylation at Thr^{545} is critical for H,K-ATPase relocation to the apical plasma membrane. As a control, the basolateral membrane marker Na,K-ATPase did not exhibit any relocation in response to histamine stimulation (Fig. 6*B*, *bottom panel*).

To quantify the translocation of the α subunit of H,K-ATPase in response to histamine stimulation, we carried out densitometric analyses of the α subunit of H,K-ATPase proteins from the plasma membrane fraction P1 and tubulovesicle fraction P3 from resting and secreting rabbit gastric gland preparations and expressed the value as the P1/P3 ratio. Quantification of the α subunit of H,K-ATPase exhibits a characteristic translocation typically seen in histamine-stimulated secreting parietal cells (11, 18). Statistical analyses from four different preparations demonstrate that H,K-ATPase significantly translocates from the cytoplasm to the apical plasma membrane fraction in a pattern similar to that of H,K-ATPase in wild-type and phospho-mimicking ACAP4^{T545D}-expressing cells but not non-phosphorylatable ACAP4^{T545A}-expressing cells (Fig. 6*C*; **, $p < 0.01$; *, $p < 0.05$ compared with those of cimetidine treatment). These results demonstrate that phosphorylation of ACAP4 Thr^{545} is essential for translocation of H,K-ATPase to the apical plasma membrane of parietal cells in response to histamine stimulation.

Discussion

Ezrin, a founding member of the membrane–cytoskeleton linker of the ezrin/radixin/moesin protein family, is essential for regulated plasma membrane–cytoskeletal dynamics underlying cell migration, immunological synapse formation, and polarized secretion (4, 23). Our early study revealed that ACAP4, an ARF6 GAP containing a pleckstrin homology domain and ankyrin repeats, interacts with ezrin and plays an essential role in acid secretion (12). Although our early study revealed that ezrin and ACAP4 form a volatile membrane regulatory complex upon histamine stimulation, the precise regu-

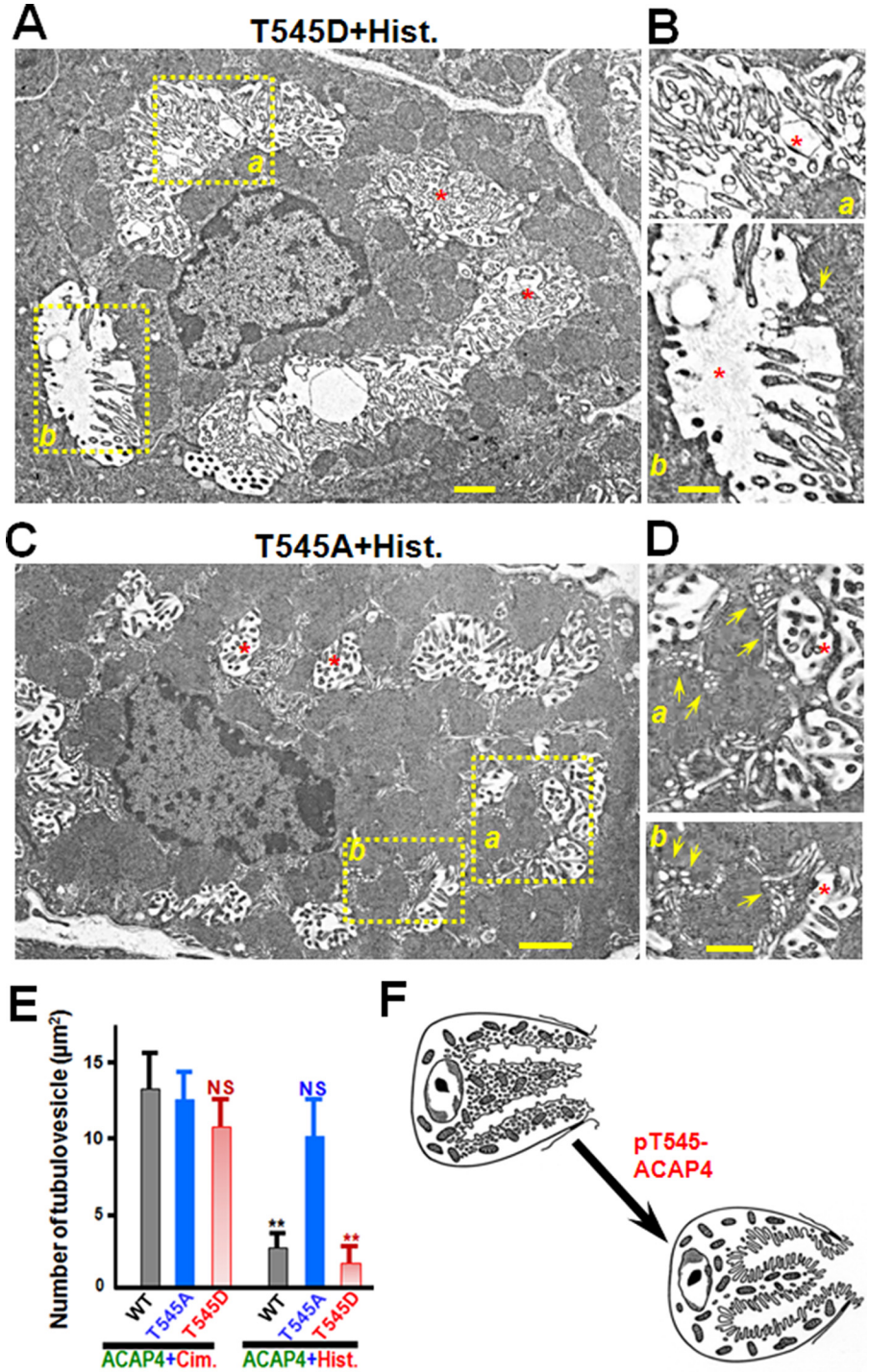

Figure 5. Phosphorylation of ACAP4 by MST4 enables recruitment of tubulovesicles to the apical membrane of parietal cells. *A*, in the resting cell, short apical microvilli are supported by long microfilaments extending deep into the cytoplasm. Stimulation leads to docking and fusion of H,K-ATPase–rich tubulovesicles to the apical plasma membrane, greatly expanding the apical surface. Interactions between the apical membrane and microfilaments, via ezrin–ACAP4 interaction, were postulated to reorganize the expanded surface into long microvilli. Aliquots of cultured parietal cells were transiently transfected to express GFP–ACAP4^{T545A} and GFP–ACAP4^{T545D} mutants, followed by histamine stimulation. The preparations were processed for classic transmission electron microscopic analyses as described under "Experimental procedures." Thin sections were post-stained with uranyl acetate and lead citrate and examined under an electron microscope. In histamine-elicited secreting parietal cells expressing ACAP4^{T545D}, the greatly expanded apical membrane is lined with numerous elongated microvilli. *Scale bar* = 1 μm. *B*, magnified view of *A* (*insets*, *a* and *b*) showing the elongation of microvilli in proximity to the microvillar membrane in parietal cells with concurrent diminished tubulovesicles. Only a few tubulovesicles can be found after careful examination (*b*, *arrow*). *Scale bar* = 500 nm. *C*, in histamine-treated parietal cells expressing ACAP4^{T545A}, short apical microvilli were evident as long microfilaments extending deep into the cytoplasm, reminiscent of non-secreting cells. *Scale bar* = 1 μm. *D*, magnified view of *C* (*insets*, *a* and *b*) showing the abundance of tubulovesicles in proximity to the microvillar membrane in parietal cells with concurrent minimized apical canalicular expansion (*). Dozens of tubulovesicles were readily apparent in parietal cells expressing ACAP4^{T545A} (*a* and *b*, *arrows*). *Scale bar* = 500 nm. *E*, quantitative analyses of tubulovesicle density in parietal cells expressing ACAP4^{T545A} and ACAP4^{T545D}, respectively. *Error bars* represent S.E.; $n = 10$. **, $p < 0.01$; *NS*, no significant difference. *Cim.*, cimetidine; *His.*, histamine. *F*, schematic illustrating the role of phosphorylation of ACAP4 at Thr^{545} in promoting the fusion of tubulovesicles to the apical membrane of parietal cells upon MST4 activation by histamine.

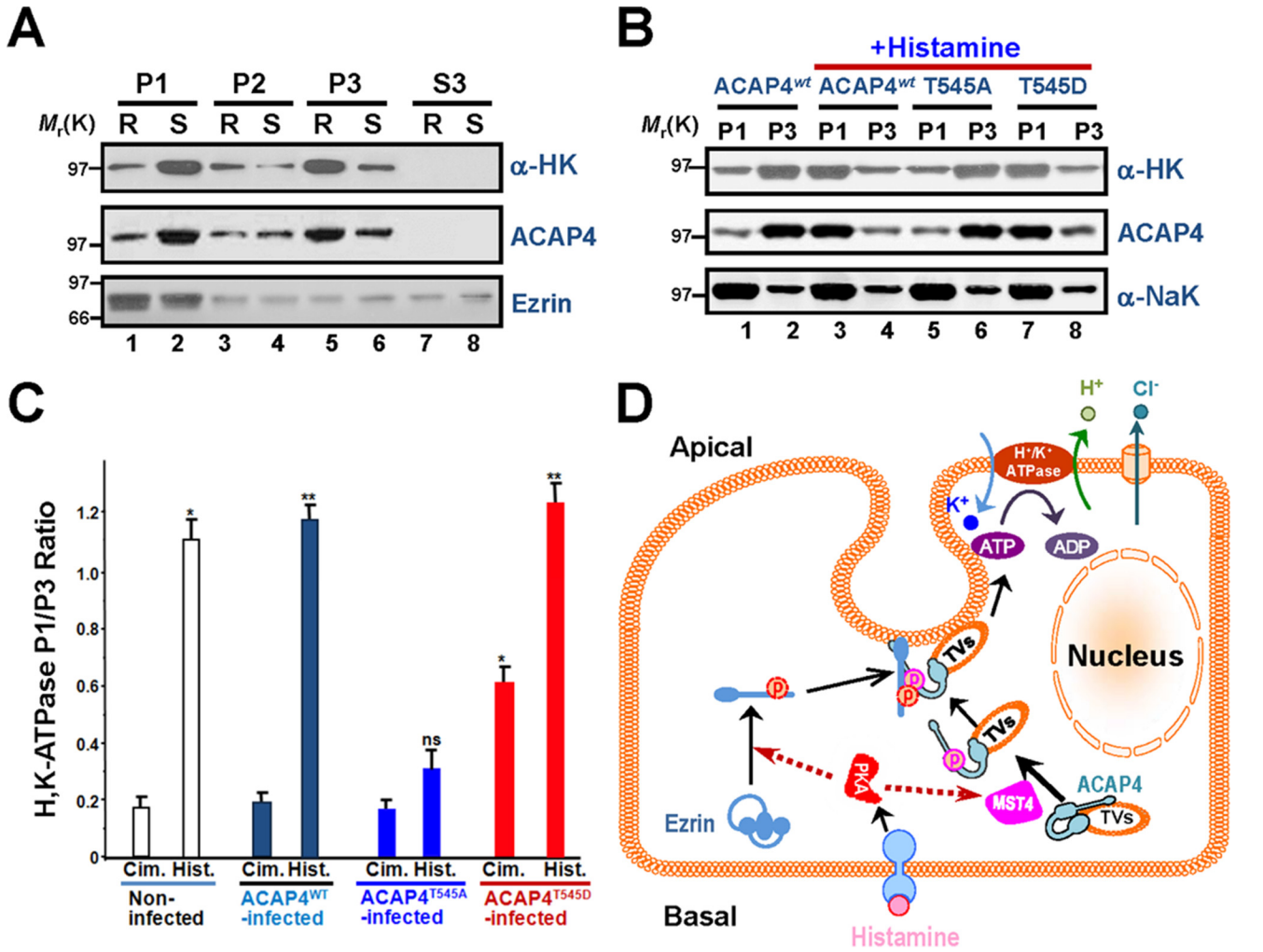

Figure 6. Phosphorylation of ACAP4 by MST4 elicited relocation of proton pump H,K-ATPase to the apical membrane of parietal cells. *A*, Western blot analyses of ACAP4, ezrin, and H,K-ATPase (α subunit) of subcellular fractions derived from resting (*R*, cimetidine) and stimulated (*S*, histamine) gastric glands. Note that stimulation enriches the protein level of H,K-ATPase (α subunit) in the P1 fraction. *B*, Western blot analyses of ACAP4, Na,K-ATPase (α subunit), and H,K-ATPase (α subunit) of subcellular fractions derived from resting and stimulated gastric glands infected with GFP–ACAP4 adenovirus (wild-type, ACAP4-T545A, and ACAP4-T545D). *C*, quantification of the α subunit of H,K-ATPase proteins from P1 (plasma membrane–enriched) and P3 (tubulovesicle-enriched) fractions. The measurements are expressed as the P1/P3 ratio. All data are given as means ± S.E. (*error bars*) of four preparations. *Cim.*, cimetidine; *Hist.*, histamine. *, $p < 0.05$; **, $p < 0.01$. *D*, working model illustrating how histamine stimulation–elicited PKA–MST4 signaling induces ezrin and ACAP4 conformational change, which enables the association of ACAP4 with ezrin and provides a spatial cue for tubulovesicle translocation. In non-secreting parietal cells, ACAP4 resides on tubulovesicles and relocates apically upon histamine stimulation. Histamine stimulation induces MST4 activation that phosphorylates ACAP4 at Thr^{545}. In addition, phosphorylation of ACAP4 promotes its association with ezrin phosphorylated at Ser^{66} by PKA (11, 18). Phosphorylation of Ser^{66} elicits a conformational change of ezrin, which promotes docking and anchoring of ACAP4-containing tubulovesicles at the apical membrane for subsequent fusion of H,K-ATPase–containing vesicles to the apical membrane for the proton pump.

lation of their physical interaction was never demonstrated. Here we provide the first evidence that MST4 phosphorylates Thr^{545} of ACAP4, which synergizes with the phosphorylation of ezrin at Ser^{66} during parietal cell activation by histamine. The PKA–MST4–ACAP4-ezrin signaling axis is important for parietal cell activation. Thus, our data provide direct evidence for a phosphorylation-coupled molecular switch of ACAP4 in operating apical membrane reorganization during regulated acid secretion in gastric parietal cells (Fig. 6*D*).

During epithelial cell polarization, cells specify their functional domains at the apical and basolateral membrane. The LKB1–STRAD–MO25 complex exhibits an essential role in epithelial cell polarity establishment (24). MST4, as an integral orchestrator of the LKB1–STRAD–MO25 signaling complex, specifically controls the formation of brush borders at the apical domain but exhibits no effect on polarization *per se* (3). Our recent study revealed the mechanism of action underlying PKA-elicited MST4 activation during parietal cell activation (11). Interestingly, MST4 translocates to the apical membrane in response to histamine stimulation because of recruitment of the vesicular membrane. Given the constitutive localization of ezrin at the apical membrane and MST4-elicited ACAP4 binding to ezrin, it would be of great interest to examine MST4 enrichment at the apical membrane via its interaction with ACAP4. Molecular delineation of the hierarchical interaction in the MST4–ezrin–ACAP4 complex will better our understanding of polarity establishment and maintenance in gastric parietal cells during the secretory cycle.

Gastric ezrin was initially identified as a PKA substrate associated with parietal cell acid secretion (25). Our recent study

shows that pSer[66] provides a spatiotemporal cue for tubulovesicle membrane trafficking to the apical membrane via a site-specific phosphorylation-coupled ezrin–syntaxin 3 interaction (18). It is worth noting that ezrin is an interacting protein of the regulatory subunit of PKA that is implicated in the apical localization of PKA (16). Thus, the interaction between phospho-ezrin and ACAP4 established here, together with a previously characterized ezrin–syntaxin 3 interaction, may organize an apical signaling, docking, and anchoring complex that orchestrates vesicular membrane recruitment and membrane cytoskeletal reorganization. Further fine mapping of respective binding interfaces between the aforementioned proteins will aid in delineating the molecular mechanisms underlying polarity establishment and polarized secretion in gastric parietal cells. In addition, it would be of great interest to visualize the spatiotemporal dynamics of MST4 kinase activity in response to histamine stimulation using a FRET-based optical sensor, given the availability of chemical inhibitor hesperadin (26). It would be equally important to see how MST4 phosphorylation of Thr[545] operates the conformational changes of ACAP4, as judged by the distance between the GAP domain and the first ankyrin repeat.

Phosphorylation of ezrin has been functionally linked to membrane dynamics and plasticity. We have recently established a protocol in which phosphorylation-mediated protein conformational change can be studied at the single-molecule level using an atomic force microscope (27). Using this protocol, we correlated the phosphorylation-induced conformational change of ezrin-Thr[567] with its functional activity in cellular localization. Using the same protocol, we show that phosphorylation of ezrin at Ser[66] also unfolds ezrin intramolecular association. Future studies will be directed to see how a single molecule of ACAP4 is unfolded in real time in response to MST4 phosphorylation. It would be equally important to carry out fine comparative analyses using photoactivation localization microscopy to delineate how phosphorylation-coupled protein conformational change is used as a signaling scaffold to orchestrate cellular dynamics (28, 29).

Aberrant acid secretion has been seen in the development of peptide ulcers, and correction of aberrant acid production promotes the recovery of patients from peptic ulcers. The current regimens aim for chemical inhibitors to block histamine binding to H2R or inhibiting proton pump activity. The importance of MST4 kinase activity for optimal acid secretion in parietal cells established here provides insight into better management of aberrant acid secretion using MST4 pharmacological inhibitors such as hesperadin (17). Interestingly, hesperadin was initially identified by its inhibitory activity toward Aurora B (30). Given the observation that Aurora kinase promotes inflammation and tumorigenesis in mice and human gastric neoplasia, it would be exciting to examine whether MST4 kinase is hyperactivated and hyperphosphorylated in gastric inflammation elicited by *Helicobacter pylori* and gastric neoplasia.

Taken together, this work reveals that MST4 interacts with and phosphorylates the tubulovesicle membrane trafficking regulator ACAP4. Phosphorylation of ACAP4 at Thr[545] promotes its association with ezrin prephosphorylated at Ser[66] by PKA. Finally, we show that phosphorylation of Thr[545] promotes the recruitment of tubulovesicles to the apical membrane and concurrent membrane–cytoskeletal reorganization essential for H,K-ATPase insertion into the plasma membrane. We propose that the MST4–ACAP4–ezrin signaling axis orchestrates phosphorylation-coupled conformational change of ACAP4 and provides a spatial control for H,K-ATPase docking at the apical membrane of gastric parietal cells.

Experimental procedures

Affinity purification of ACAP4 and mass spectrometric identification of ACAP4 phosphorylation sites

To characterize the histamine-elicited protein interaction between ACAP4 and MST4, an anti-ACAP4 antibody affinity matrix was prepared as described previously (12, 15). Briefly, the ACAP4 mouse antibody 2D6 was dialyzed against distilled water and 0.1 M HEPES (pH 8.0). The beads were gently mixed with 2D6 for 4 h at 4 °C. The 2D6 antibody–coupled beads were washed with PBS and then incubated with 1 M ethanolamine (pH 8.0) for 1 h to block excess unreacted *N*-hydroxysuccinimide groups. The affinity column was stored at 4 °C in PBS containing 0.1% NaN_3. Before each run, the column was washed with elution buffer and re-equilibrated with PBS before applying gastric membrane extracts as described previously (18).

The gastric membrane fraction from the histamine-stimulated preparation, containing large organelles including apical plasma membrane fragments enriched in ACAP4, ezrin, and H,K-ATPase (12), was extracted with extraction buffer containing 0.25% Triton X-100, 200 mM NaCl, 1 mM EGTA, 20 mM Tris-Cl (pH 7.4), and protease inhibitor mixture (Sigma) on ice for 30 min and centrifuged at 20,000 × *g* for 20 min. Aliquots of the supernatant were mixed by gentle rotation for 2 h at 4 °C with affinity matrix coupled with anti-ACAP4 antibody. The proteins bound on the affinity matrix were then eluted with 0.2 M glycine (pH 2.3), followed by 75% ethanol precipitation at −20 °C for 1 h. The precipitated proteins were then reconstituted in SDS-PAGE sample buffer and subjected to electrophoresis and immunoblotting analyses. To pinpoint the phosphorylation sites on ACAP4 associated with parietal cell activation, the ACAP4 protein band was cut from the aforementioned SDS-PAGE and subjected to trypsin in-gel digestion, followed by mass spectrometric analyses as described previously (13).

Isolation of gastric glands and AP uptake assay

Gastric glands were isolated from New Zealand White rabbits as modified by Yao *et al.* (7). Briefly, the rabbit stomach was perfused under high pressure with PBS (2.25 mM K_2HPO_4, 6 mM Na_2HPO_4, 1.75 mM NaH_2PO_4, and 136 mM NaCl (pH 7.4)) containing 1 mM $CaCl_2$ and 1 mM $MgSO_4$. The gastric mucosa was scraped from the smooth muscle layer, minced, and then washed twice with minimal essential medium (MEM) buffered with 20 mM HEPES (pH 7.4) (HEPES–MEM). The minced mucosa was then digested with 15 mg of collagenase (Sigma-Aldrich, St. Louis, MO). Intact gastric glands were collected from the digestion mixture for 20–25 min and then washed three times in HEPES–MEM. In all subsequent gland experiments (AP uptake assay), glands were resuspended at 5% cytocrit (v/v) in the appropriate buffer containing histamine

receptor 2 blockers (cimetidine or famotidine, 5 μM) for the final assay.

Stimulation of intact and Streptolysin O (SLO, Sigma-Aldrich)-permeabilized rabbit gastric glands was quantified using the AP uptake assay, as described by Ammar *et al.* (19). Briefly, intact glands in HEPES–MEM were washed twice by settling at 4 °C in ice-cold K buffer (10 mM Tris base, 20 mM HEPES acid, 100 mM KCl, 20 mM NaCl, 1.2 mM $MgSO_4$, 1 mM NaH_2PO_4, and 40 mM mannitol (pH7.4)). SLO was added to a final concentration of 1 μg/ml, and the glands (at 5% cytocrit) were mixed by inversion and then incubated on ice for 10 min. The glands were then washed twice with ice-cold K buffer to remove unbound SLO, and permeabilization was initiated by incubating the gland suspension at 37 °C in K buffer solution containing 1 mM pyruvate and 10 mM succinate. Stimulation of intact gastric glands was achieved either by histamine (100 μM) plus IBMX (50 μM, Sigma-Aldrich) or by a membrane-permeable analogue of cAMP, such as dibutyl cAMP (1 mM, Sigma-Aldrich) at 20-min intervals.

Cell culture and transfection

Primary cultures of gastric parietal cells from rabbit stomach were produced and maintained as described previously (5). Separate cultures of parietal cells were transfected with plasmids encoding GFP-tagged wild-type ACAP4 and/or mutants using Lipofectamine 2000 (Invitrogen) according to the instructions of the manufacturer. Briefly, 1 μg of DNA was incubated in 600 μl of Opti-MEM (antibiotic-free), and then 6 μl of Lipofectamine 2000 was added and left at room temperature for 25 min. The cultured parietal cells (~3% cytocrit; 6-well plates) were washed once with Opti-MEM. The DNA–lipid mixture was added to the plates and incubated for 4 h, followed by replacement of 1.5 ml of DMEM/F-12 medium (Gibco) (medium B). The transfected cells were then maintained in culture at 37 °C until use for protein expression, partition, immunoprecipitation, or immunofluorescence.

Infection of cultured parietal cells with adenoviral GFP-ACAP4, GFP-ACAP4^{T545A}, and GFP-ACAP4^{T545D} was described previously (18, 31, 32). The infection efficiency and expression levels of various ezrin proteins exhibit no difference among different variants. MST4 and ACAP4 siRNA, whose targeted sequence was the same as described previously (11, 12), was synthesized by Qiagen.

Preparation of gastric subcellular fractions

Gastric subcellular fractions were prepared according to Jiang *et al.* (11). All fractionation procedures were performed under ice-cold conditions. Briefly, the treated glands were rinsed once in homogenizing buffer containing 125 mM mannitol, 40 mM sucrose, 1 mM EDTA, and 5 mM PIPES-Tris (pH 6.7) and homogenized with a very tightly fitting Teflon pestle. The homogenate was centrifuged to produce a series of pellets: P0, 40 × *g* for 5 min (whole cells and debris); P1, 4000 × *g* for 10 min (plasma membrane–rich fraction); P2, 14,500 × *g* for 10 min; P3, 100,000 × *g* for 60 min (microsomes); and S3, supernatant (cytosol). The pellets were resuspended in medium containing 300 mM sucrose, 0.2 mM EDTA, and 5 mM Tris (pH 7.4). The protein concentration in each individual subcellular fraction was assayed using bovine serum albumin as a standard (11).

Purification of recombinant ezrin proteins

Recombinant wild-type ezrin, together with its phosphomimicking (S66D) and non-phosphorylatable (S66A) mutants, was expressed in bacteria as His_6-tagged fusion proteins exactly as described previously (27). Purified ezrin was eluted with 250 mM imidazole and then applied to a gel filtration column to remove imidazole. The fusion protein was estimated to be of 90–95% purity, as judged by SDS-PAGE; the major contaminants were degraded fragments of ezrin. Protein concentration was determined by Bradford assay.

Recombinant wild-type ACAP4, together with its phospho-mimicking (T545D) and non- phosphorylatable (T545A) mutants, was expressed in bacteria as His_6- or GST-tagged fusion proteins exactly as described previously (27). The fusion protein was estimated to be of 89–93% purity, as judged by SDS-PAGE; the major contaminants were degraded fragments of ACAP4. Protein concentration was determined by Bradford assay.

[^{14}C]AP uptake assay

Stimulation of parietal cells was quantified using the AP uptake assay as described previously (20). Cells were transfected with ACAP4 wild-type and mutants (T545A and T545D) 36 h before stimulation of histamine and IBMX (100 and 30 μM, respectively). AP uptake values were normalized among the various preparations by expressing as a fraction of the maximally stimulated control. In some cases, an aliquot of parietal cells was pretreated with 20 nM hesperadin (an MST4 inhibitor) at 37 °C for 10 min, followed by histamine stimulation at 37 °C for an additional 20 min to judge the function of MST4 in parietal cell secretion. To examine whether histamine-stimulated and MST4-mediated parietal cell secretion depends on proton pump H,K-ATPase, aliquots of parietal cells were treated with omeprazole (Sigma, 100 nM), an H,K-ATPase inhibitor, as described previously (11).

In vitro phosphorylation

The kinase reactions were performed in 40 μl of 1× kinase buffer (25 mM HEPES (pH 7.2), 50 mM NaCl, 2 mM EGTA, 5 mM $MgSO_4$, 1 mM DTT, and 0.01% Brij35), casein or various recombinant ACAP4 proteins (2 μg) as substrate, purified MST4 (5–10 ng) as kinase, 5 μCi of [γ-^{32}P]ATP, and 500 μM ATP. Reaction mixtures were incubated at 30 °C for 30 min and then stopped by SDS sample buffer. Proteins were resolved by SDS-PAGE. Gels were dried and exposed, and ^{32}P incorporation into casein proteins was quantified by PhosphorImager (Amersham Biosciences).

Immunofluorescence

Some cultured parietal cells were treated with 100 μM cimetidine to maintain a resting state; others were treated with the secretory stimulants 100 μM histamine plus 50 μM IBMX in the presence of SCH28080, a proton pump inhibitor (5). Treated cells were then fixed with 2% formaldehyde for 10 min, washed three times with PBS, followed by permeabilization in 0.1% Triton X-100 for 5 min. Prior to application of primary antibody, the fixed and permeabilized cells were blocked with 0.5% BSA

in PBS, followed by incubation of primary antibodies against ACAP4 and MST4, respectively. The endogenous ACAP4 proteins were labeled by a rhodamine-conjugated goat anti-mouse antibody and counterstained with MST4, which was labeled with FITC-conjugated goat anti-rabbit antibody (Jackson ImmunoResearch Laboratories). Coverslips were supported on slides by grease pencil markings and mounted in Vectashield mounting medium (Vector Laboratories).

Confocal microscopy

Immunostained parietal cells were examined under a laser-scanning confocal microscope (LSM510 NLO, Carl Zeiss) scan head mounted transversely to an inverted microscope (Axiovert 200, Carl Zeiss) with a 40 × 1.0 numerical aperture (NA) PlanApo objective. Single images were collected by an average of 10 scans at a scan rate of 1 s/scan. Optical section series were collected with a spacing of 0.4 μm in the z axis through the ~12-μm thickness of the cultured parietal cells. The images of double labeling were collected simultaneously using a dichroic filter set with Zeiss image processing software (LSM 5, Carl Zeiss). Digital data were exported into Adobe Photoshop for presentation.

Pulldown assays

Recombinant proteins with GST or His_6 tag were expressed and purified as described previously (33). For pulldown analyses, His_6–ezrin fusion proteins on agarose beads were incubated with appropriate GST–ACAP4 proteins at 4 °C for 2 h. The resins were washed extensively, followed by SDS-PAGE and Western blot analyses.

Electron microscopy

Isolated gastric glands were infected with adenoviral-ACAP4^{T545A} and ACAP4^{T545D} prior to histamine stimulation. These treated glands were then fixed in 2% glutaldehyde (Tousimis) in PBS and processed as described previously (8, 20). Thin serial sections (silver–gold) were then cut, post-stained, and examined with a JEOL 1200 electron microscope.

Western blot

Samples were subjected to SDS-PAGE on 6–16% gradient gel and transferred onto nitrocellulose membranes. Proteins were probed by appropriate primary antibodies and detected using ECL (Pierce). The band intensity was then quantified using ImageJ (National Institutes of Health).

Computational analyses and molecular modeling

ACAP4–ARF6 structures (PDB code 3LVR) were analyzed and presented. Briefly, because of the flexibility of the linker (Val^{536}–Glu^{547}), the crystal structure of the ACAP4–ARF6 complex (PDB code 3LVR) contains a chain break at the Thr^{545} region. To fix the missing residues, we entered the loop sequence VEHRFARRCTPE (Val^{536}–Glu^{547} of ACAP4) into the online sever RCD+ (http://rcd.chaconlab.org/)[7] (34) and generated the 20 best energy all-atom loop structures. The lowest-energy loop was selected to bridge the gap in the final structure model by PyMOL software (35). The complex structure was derived from the ACAP4–ARF6 complex (PDB code 3LVR), whereas the loop annotated by the yellow peptide was generated by RCD+ online sever.

Data analyses

All fluorescence intensity measurements were carried out using MetaMorph software. Maximal projected images were used for these measurements. The relative fluorescence intensity of various ACAP4 mutants at the apical membrane was calculated and expressed as ratio of ACAP4 signal over F-actin signal, which was stained by Alexa Fluor 647 Phalloidin (Thermo Fisher). To determine significant differences between means, unpaired t tests assuming unequal variance were performed; differences were considered significant when $p < 0.05$.

Author contributions—X. L., X. D., and X. Yao conceived the project. X. Yuan, P. Y. Y., J. J., Y. Z., Z. S., X. W., P. G., X. Z., and F. W. designed and performed most biochemical experiments. X. Yuan, W. Y., T. W., M. M., C. H., W. W., D. W., X. L., and X. D. designed and performed cell biological characterization. X. Yuan, R. T., L. B., X. C., and X. D. performed the *in vitro* reconstitution experiment and data analyses. All authors contributed to the writing or editing of the manuscript.

Acknowledgments—We thank Dr. John G. Forte for the visionary theory of the membrane recruitment and recycling model of H,K-ATPase activation illustrated in Fig. 5F, Dr. Zhenwei Song for assistance with computation of the ACAP4 molecular structure, and Dr. Jiajia Zhou for assistance with diagram drawing. We also thank the members of our groups for stimulating discussions.

References

1. Yao, X., and Forte, J. G. (2003) Cell biology of acid secretion by the parietal cell. *Annu. Rev. Physiol.* **65,** 103–131
2. Rawat, S. J., and Chernoff, J. (2015) Regulation of mammalian Ste20 (Mst) kinases. *Trends Biochem. Sci.* **40,** 149–156
3. ten Klooster, J. P., Jansen, M., Yuan, J., Oorschot, V., Begthel, H., Di Giacomo, V., Colland, F., de Koning, J., Maurice, M. M., Hornbeck, P., and Clevers, H. (2009) Mst4 and Ezrin induce brush borders downstream of the Lkb1/Strad/Mo25 polarization complex. *Dev. Cell* **16,** 551–562
4. Bretscher, A., Edwards, K., and Fehon, R. G. (2002) ERM proteins and merlin: integrators at the cell cortex. *Nat. Rev. Mol. Cell Biol.* **3,** 586–599
5. Zhou, R., Cao, X., Watson, C., Miao, Y., Guo, Z., Forte, J. G., and Yao, X. (2003) Characterization of protein kinase A-mediated phosphorylation of ezrin in gastric parietal cell activation. *J. Biol. Chem.* **278,** 35651–35659
6. Nakamura, F., Amieva, M. R., and Furthmayr, H. (1995) Phosphorylation of threonine 558 in the carboxyl-terminal actin-binding domain of moesin by thrombin activation of human platelets. *J. Biol. Chem.* **270,** 31377–31385
7. Yao, X., Chaponnier, C., Gabbiani, G., and Forte, J. G. (1995) Polarized distribution of actin isoforms in gastric parietal cells. *Mol. Biol. Cell* **6,** 541–557
8. Yao, X., Cheng, L., and Forte, J. G. (1996) Biochemical characterization of ezrin-actin interaction. *J. Biol. Chem.* **271,** 7224–7229
9. Hanzel, D. K., Urushidani, T., Usinger, W. R., Smolka, A., and Forte, J. G. (1989) Immunological localization of an 80-kDa phosphoprotein to the apical membrane of gastric parietal cells. *Am. J. Physiol.* **256,** G1082–G1089
10. Tamura, A., Kikuchi, S., Hata, M., Katsuno, T., Matsui, T., Hayashi, H., Suzuki, Y., Noda, T., Tsukita, S., and Tsukita, S. (2005) Achlorhydria by

[7] Please note that the JBC is not responsible for the long-term archiving and maintenance of this site or any other third party–hosted site.

ezrin knockdown: defects in the formation/expansion of apical canaliculi in gastric parietal cells. *J. Cell Biol.* **169,** 21–28

11. Jiang, H., Wang, W., Zhang, Y., Yao, W. W., Jiang, J., Qin, B., Yao, W. Y., Liu, F., Wu, H., Ward, T. L., Chen, C. W., Liu, L., Ding, X., Liu, X., and Yao, X. (2015) Cell polarity kinase MST4 cooperates with cAMP-dependent kinase to orchestrate histamine-stimulated acid secretion in gastric parietal cells. *J. Biol. Chem.* **290,** 28272–28285
12. Ding, X., Deng, H., Wang, D., Zhou, J., Huang, Y., Zhao, X., Yu, X., Wang, M., Wang, F., Ward, T., Aikhionbare, F., and Yao, X. (2010) Phospho-regulated ACAP4-Ezrin interaction is essential for histamine-stimulated parietal cell secretion. *J. Biol. Chem.* **285,** 18769–18780
13. Zhao, X., Wang, D., Liu, X., Liu, L., Song, Z., Zhu, T., Adams, G., Gao, X., Tian, R., Huang, Y., Chen, R., Wang, F., Liu, D., Yu, X., Chen, Y., *et al.* (2013) Phosphorylation of the Bin, Amphiphysin, and RSV161/167 (BAR) domain of ACAP4 regulates membrane tubulation. *Proc. Natl. Acad. Sci. U.S.A.* **110,** 11023–11028
14. Yu, X., Wang, F., Liu, H., Adams, G., Aikhionbare, F., Liu, D., Cao, X., Fan, L., Hu, G., Chen, Y., Frost, A., Partridge, E., Ding, X., and Yao, X. (2011) ACAP4 protein cooperates with Grb2 protein to orchestrate epidermal growth factor-stimulated integrin β1 recycling in cell migration. *J. Biol. Chem.* **286,** 43735–43747
15. Fang, Z., Miao, Y., Ding, X., Deng, H., Liu, S., Wang, F., Zhou, R., Watson, C., Fu, C., Hu, Q., Lillard, J. W., Jr., Powell, M., Chen, Y., Forte, J. G., and Yao, X. (2006) Proteomic identification and functional characterization of a novel ARF6 GTPase-activating protein, ACAP4. *Mol. Cell Proteomics* **5,** 1437–1449
16. Dransfield, D. T., Bradford, A. J., Smith, J., Martin, M., Roy, C., Mangeat, P. H., and Goldenring, J. R. (1997) Ezrin is a cyclic AMP-dependent protein kinase anchoring protein. *EMBO J.* **16,** 35–43
17. Xiong, W., Matheson, C. J., Xu, M., Backos, D. S., Mills, T. S., Salian-Mehta, S., Kiseljak-Vassiliades, K., Reigan, P., and Wierman, M. E. (2016) Structure-based screen identification of a mammalian Ste20-like kinase 4 (MST4) inhibitor with therapeutic potential for pituitary tumors. *Mol. Cancer Ther.* **15,** 412–420
18. Yu, H., Zhou, J., Takahashi, H., Yao, W., Suzuki, Y., Yuan, X., Yoshimura, S. H., Zhang, Y., Liu, Y., Emmett, N., Bond, V., Wang, D., Ding, X., Takeyasu, K., and Yao, X. (2014) Spatial control of proton pump H,K-ATPase docking at the apical membrane by phosphorylation-coupled ezrin-syntaxin 3 interaction. *J. Biol. Chem.* **289,** 33333–33342
19. Ammar, D. A., Zhou, R., Forte, J. G., and Yao, X. (2002) Syntaxin 3 is required for cAMP-induced acid secretion: streptolysin *O*-permeabilized gastric gland model. *Am. J. Physiol. Gastrointest. Liver Physiol.* **282,** G23–G33
20. Wang, F., Xia, P., Wu, F., Wang, D., Wang, W., Ward, T., Liu, Y., Aikhionbare, F., Guo, Z., Powell, M., Liu, B., Bi, F., Shaw, A., Zhu, Z., Elmoselhi, A., *et al.* (2008) *Helicobacter pylori* VacA disrupts apical membrane–cytoskeletal interactions in gastric parietal cells. *J. Biol. Chem.* **283,** 26714–26725
21. Cao, X., Ding, X., Guo, Z., Zhou, R., Wang, F., Long, F., Wu, F., Bi, F., Wang, Q., Fan, D., Forte, J. G., Teng, M., and Yao, X. (2005) PALS1 specifies the localization of ezrin to the apical membrane of gastric parietal cells. *J. Biol. Chem.* **280,** 13584–13592
22. Forte, J. G., and Yao, X. (1996) The membrane-recruitment-and-recycling hypothesis of gastric HCl secretion. *Trends Cell Biol.* **6,** 45–48
23. Fehon, R. G., McClatchey, A. I., and Bretscher, A. (2010) Organizing the cell cortex: the role of ERM proteins. *Nat. Rev. Mol. Cell Biol.* **11,** 276–287
24. Baas, A. F., Kuipers, J., van der Wel, N. N., Batlle, E., Koerten, H. K., Peters, P. J., and Clevers, H. C. (2004) Complete polarization of single intestinal epithelial cells upon activation of LKB1 by STRAD. *Cell* **116,** 457–466
25. Urushidani, T., Hanzel, D. K., and Forte, J. G. (1989) Characterization of an 80-kDa phosphoprotein involved in parietal cell stimulation. *Am. J. Physiol.* **256,** G1070–G1081
26. Chu, Y., Yao, P. Y., Wang, W., Wang, D., Wang, Z., Zhang, L., Huang, Y., Ke, Y., Ding, X., and Yao, X. (2011) Aurora B kinase activation requires survivin priming phosphorylation by PLK1. *J. Mol. Cell Biol.* **3,** 260–267
27. Liu, D., Ge, L., Wang, F., Takahashi, H., Wang, D., Guo, Z., Yoshimura, S. H., Ward, T., Ding, X., Takeyasu, K., and Yao, X. (2007) Single-molecule detection of phosphorylation-induced plasticity changes during ezrin activation. *FEBS Lett.* **581,** 3563–3571
28. Xia, P., Liu, X., Wu, B., Zhang, S., Song, X., Yao, P. Y., Lippincott-Schwartz, J., and Yao, X. (2014) Superresolution imaging reveals structural features of EB1 in microtubule plus-end tracking. *Mol. Biol. Cell* **25,** 4166–4173
29. Xia, P., Zhou, J., Song, X., Wu, B., Liu, X., Li, D., Zhang, S., Wang, Z., Yu, H., Ward, T., Zhang, J., Li, Y., Wang, X., Chen, Y., Guo, Z., and Yao, X. (2014) Aurora A orchestrates entosis by regulating a dynamic MCAK-TIP150 interaction. *J. Mol. Cell Biol.* **6,** 240–254
30. Katsha, A., Soutto, M., Sehdev, V., Peng, D., Washington, M. K., Piazuelo, M. B., Tantawy, M. N., Manning, H. C., Lu, P., Shyr, Y., Ecsedy, J., Belkhiri, A., and El-Rifai, W. (2013) Aurora kinase A promotes inflammation and tumorigenesis in mice and human gastric neoplasia. *Gastroenterology* **145,** 1312–1322.e1–e8
31. Karvar, S., Yao, X., Crothers, J. M., Jr, Liu, Y., and Forte, J. G. (2002) Localization and function of soluble *N*-ethylmaleimide-sensitive factor attachment protein-25 and vesicle-associated membrane protein-2 in functioning gastric parietal cells. *J. Biol. Chem.* **277,** 50030–50035
32. Karvar, S., Yao, X., Duman, J. G., Hybiske, K., Liu, Y., and Forte, J. G. (2002) Intracellular distribution and functional importance of vesicle-associated membrane protein 2 in gastric parietal cells. *Gastroenterology* **123,** 281–290
33. Cao, D., Su, Z., Wang, W., Wu, H., Liu, X., Akram, S., Qin, B., Zhou, J., Zhuang, X., Adams, G., Jin, C., Wang, X., Liu, L., Hill, D. L., Wang, D., *et al.* (2015) Signaling scaffold protein IQGAP1 interacts with microtubule plus-end tracking protein SKAP and links dynamic microtubule plus-end to steer cell migration. *J. Biol. Chem.* **290,** 23766–23780
34. López-Blanco, J. R., Canosa-Valls, A. J., Li, Y., and Chacón, P. (2016) RCD+: fast loop modeling server. *Nucleic Acids Res.* **44,** W395–W400
35. DeLano, W. L. (2012) *The PyMOL Molecular Graphics System*, version 1.5.0.1, Schroedinger, LLC, New York